Springer

KSME

Journal of Mechanical Science and Technology 29 (1) (2015) 251~258
www.springerlink.com/content/1738-494x
DOI 10.1007/s12206-014-1231-y

# Effect of guide vanes on recovering uniform flow in a ventilation duct in an existing twin-track subway tunnel †

Makhsuda Juraeva[1], Kyung Jin Ryu[1], Sang-Hyun Jeong[2] and Dong Joo Song[1,*]

[1]*School of Mechanical Engineering, Yeungnam University, Geyongsan-si, 712-749, Korea*
[2]*Korea Institute of Machinery and Materials, Daejeon, Korea*

(Manuscript Received February 10, 2014; Revised August 19, 2014; Accepted October 1, 2014)

**Abstract**

The steady three-dimensional airflow in a subway tunnel was analyzed using ANSYS CFX software by solving Reynolds-averaged Navier-Stokes equations. A ventilation system in a model subway tunnel was developed by analyzing the mass flow rate through the ventilation shafts and the airflow in the tunnel. The airflow in the tunnel and mass flow rate in the shafts were investigated with a guide vane, porous zone, and air-curtain installed in the subway model tunnel. A mechanical shaft of an existing subway tunnel in Seoul was analyzed to apply the developed ventilation system to the tunnel. The ducts of the mechanical shaft were connected in two different ways, and guide vanes were installed in the shafts. An emergency duct between the ducts of the mechanical shaft was used to connect the ducts and install the precipitator. An axial flow fan in the duct was used to induce swirling flow. Guide vanes were installed at one side and both sides of the shaft before the electric precipitator to obtain uniform flow, which enhances the performance of the precipitator. A proper duct connection for higher mass flow rate was obtained. The installation of guide vanes on both sides led to more uniform flow in the duct. The developed ventilation system was applied to the actual subway tunnel by connecting ducts and installing the guide vanes on both sides of the ducts.

*Keywords*: Indoor air quality; Guide vane; Mechanical shaft; Subway tunnel; Train-induced flow

## 1. Introduction

Subway tunnels and ventilation systems are in enclosed spaces, and the air quality deteriorates due to air pollutants emitted from moving trains. High-performance trains generate substantial amounts of heat and dust that exceed the amount that can be discharged with piston-effect ventilation from the subway tunnel. Proper subway ventilation is needed to maintain indoor air quality (IAQ). Platform screen doors (PSDs) improve the platform environment, but they may degrade the air quality in the subway tunnel. The particulate matter (PM) level is higher in the tunnel than on the subway platform. The major chemical species in the subway are Fe-containing, carbonaceous, soil-derived particles, and aerosols such as nitrates and sulfates. The indoor air of a subway contains heavy metal PM generated from the friction of the wheels and brake pads. Gaseous nitrogen and sulfur oxides are abundant in the indoor environment of the subway. The airborne radon levels in the subway cabins were increased by 53% after PSD installation in subway stations [1]. Radon is a colorless, odorless, and tasteless gas produced by radioactive decay of uranium and thorium, and its products are health hazards.

Experimental and numerical studies have been performed to analyze the unsteady three-dimensional flow field in tunnels with a single track [2, 3]. The train-induced airflow was also studied both numerically and experimentally for tunnels with more than one track. Experimental studies investigating the effects of moving vehicles on the tunnel ventilation were performed for two trains moving in the same direction and opposite directions [4]. The airflow was not sufficient to push vitiated air out of the tunnel when two trains ran in opposite directions. Numerical simulations were performed to analyze the airflow in a twin-track subway tunnel [5, 6]. An adequate subway ventilation system is necessary to maintain the IAQ [7]. The station IAQ becomes worse due to high concentrations of the fine dust that is transported to the subway platform by trains in the tunnels. Therefore, a proper ventilation system is needed to maintain IAQ in a subway tunnel [8].

A model subway tunnel was constructed to develop a tunnel ventilation system. The objective of this study was to find a proper ventilation system for the model tunnel, and to apply this ventilation system to an existing subway tunnel. The airflows in the model subway tunnel and the existing subway

*Corresponding author. Tel.: +82 053 810 2449, Fax.: +82 053 810 4627
E-mail address: djsong@yu.ac.kr
† Recommended by Associate Editor Seongwon Kang

tunnel were analyzed using ANSYS CFX software by solving Reynolds-averaged Navier-Stokes equations [9].

## 2. Computational procedure

### *2.1 The model subway tunnel: the computational domain and experiment*

The ventilation system of a model subway tunnel was investigated numerically and experimentally. The model subway tunnel was 54 m long, 1.65 m high, and 2.5 m wide. The tunnel was a one-quarter scale model of a real subway tunnel. The tunnel had three U-type mechanical ventilation shafts, as shown in Fig. 1. Each ventilation shaft had two axial-flow fans: one for discharging air and the other for supplying air to the tunnel. The air is discharged to the shafts through the axial-flow suction fan of each ventilation shaft, and the cleaned air enters the tunnel through the installed axial-flow fan.

An air-curtain nozzle was installed between the ducts of the ventilation shaft of the subway tunnel [10]. The thickness and length of the air-curtain nozzle were fixed to 0.1 m and 1.4 m, respectively. A guide vane was installed at the end of the ducts of the ventilation shafts. The installation angle of the guide vane was 60° [11]. The electric precipitator in the middle of each ventilation shaft has filtering media with an effective filtration process. Simulated air currents from trains were generated artificially by using an axial-flow fan at the tunnel inlet.

### *2.2 The boundary conditions and grid validation*

The computational grid of the model subway tunnel was generated using an unstructured grid. The grid was distributed along the X, Y, and Z axes. A grid validation study was performed to ensure that the computed quantities would properly converge. The number of elements in the tetrahedral mesh was between 850,000 and 1,600,000. The airflow passing through the shaft was measured in the tunnel. Grid convergence test results indicated that the proper number of elements for the tunnel flow study at which the mass flow rate passing through the shaft converged to an almost constant value was approximately 1,000,000 as shown in Fig. 2. The minimum grid size was 0.001 m, and the maximum grid size was 0.01 m based on the converged solutions.

A numerical computation was performed without train runs. The working fluid was air at 25 °C under atmospheric pressure. Adiabatic wall boundary condition was used for the tunnel walls, as shown in Table 1. All walls were treated as viscous adiabatic surfaces with no-slip velocity conditions. Open conditions were imposed at the outlet of the subway model tunnel. The pressure boundary conditions were applied to the ducts of the shafts. An air-curtain velocity of 25 m/s was applied at the air-curtain inlet. The flow field was analyzed in steady-state conditions. The train-wind velocity was applied to the tunnel inlet.

Table 1. Boundary conditions for the computational domain.

| Boundary condition | Location | Value |
|---|---|---|
| Inlet | Air-curtain inlet<br>Duct 1 inlet<br>Tunnel inlet | 25 m/s<br>196.2 Pa<br>4 m/s |
| Outlet | Duct 2 inlet | 196.2 Pa |
| Opening | Tunnel outlet | 0 Pa |
| Wall | Tunnel wall | No-slip, adiabatic |

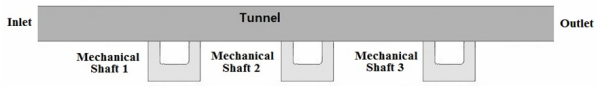


Fig. 1. Schematic view of the computational domain of the model tunnel (top view).

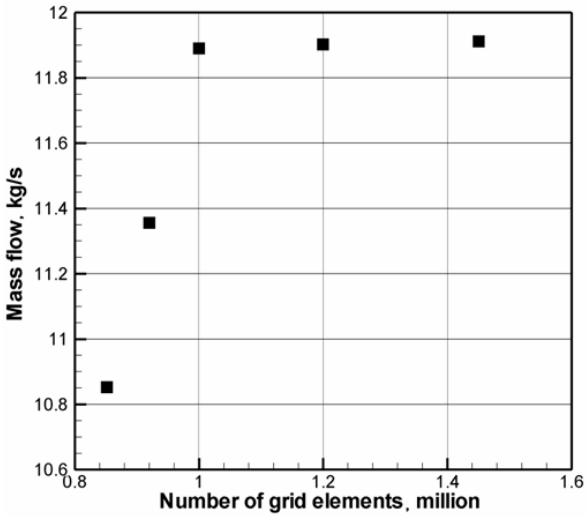


Fig. 2. Grid convergence test results with the mass flow rate and number of grid elements.

### *2.3 The computational tools and turbulence model*

ANSYS CFX software includes Workbench, CFX-Pre, CFX-Solver, and CFX-Post. The ANSYS Workbench can be used to provide the geometry or to modify the geometry provided in other data formats. Standard two-equation turbulence models often fail to predict the onset and the amount of flow separation under adverse pressure-gradient conditions, but the k-ω-based shear stress transport (SST) model was designed to make highly accurate predictions of the onset and the amount of flow separation under adverse pressure gradients by the inclusion of transport effects into the formulation of the eddy viscosity [12]. The choice of the turbulence model depends on the flow physics, including massive flow separations, as well as the established practices for a specific class of problem, the level of accuracy required, the available computational resources, and the amount of computing time available for the simulation. The *k-ω*-based SST model had similar governing equations to those of the standard *k-ω* model [13].

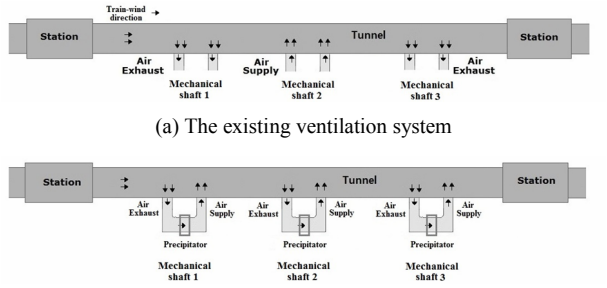


(a) The existing ventilation system

(b) The proposed ventilation system

Fig. 3. Ventilation system in the model tunnel.

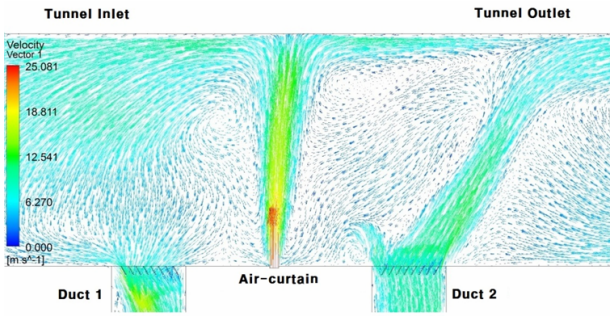


Fig. 4. The airflow distributions from the air curtain in the tunnel.

$$\frac{\partial}{\partial t}(\rho k)+\frac{\partial}{\partial x_i}(\rho k u_i)=\frac{\partial}{\partial x_i}\left(\Gamma_k\frac{\partial k}{\partial x_j}\right)+\tilde{G}_k-Y_k+S_k, \quad (1)$$

$$\frac{\partial}{\partial t}(\rho \omega)+\frac{\partial}{\partial x_i}(\rho \omega u_i)=\frac{\partial}{\partial x_i}\left(\Gamma_\omega\frac{\partial \omega}{\partial x_j}\right)+G_\omega-Y_\omega+D_\omega+S_\omega. \quad (2)$$

In Eqs. (1) and (2), $\tilde{G}_k$ represents the generation of turbulence kinetic energy due to the mean velocity gradients. $G_\omega$ represents the generation of $\omega$, which is the dissipation per unit turbulence kinetic energy. $\Gamma_k$ and $\Gamma_\omega$ are the effective diffusivities of $k$ and ω, respectively. $Y_k$ and $Y_\omega$ represent the dissipations of $k$ and $\omega$ due to the turbulence. $D_\omega$ is the cross-diffusion term. $S_k$ and $S_\omega$ are user-defined source terms.

## 3. Results and discussions

### *3.1 The ventilation systems in the model subway tunnel*

Fig. 3 shows an existing ventilation system and the proposed ventilation system in a subway tunnel. In the existing ventilation system, clean air enters the subway tunnel through mechanical shaft 2, while the dirty air is discharged through mechanical shafts 1 and 3. The dirty air is discharged through the duct fans of the mechanical shaft, and the air is cleaned by passing through the precipitator, after which the cleaned air enters the tunnel in the proposed ventilation system [14].

Experimental and numerical analyses were performed without actual train runs in the model subway tunnel. The train wind is the wake flow generated by the axial flow fan at the tunnel inlet. The air inside the tunnel was assumed to be polluted in the numerical analysis. The developed ventilation system was constructed such that the polluted air passes the electric precipitator installed at each of the mechanical shaft. The air passing through the precipitator enters the tunnel through the axial-flow fan of each mechanical shaft.

The model subway tunnel was investigated with guide vane and air-curtain installations, with a train-wind velocity of 4 m/s applied at the tunnel inlet. The guide vanes were installed at the connected parts of the mechanical shaft with the tunnel to direct the airflow. The guide vane installation angles were 60° at the ducts of each mechanical shaft. The air from ducts impinged on the opposite wall and flowed along the wall toward the tunnel outlet. An air curtain was installed between the ducts of the ventilation shafts at the side of the tunnel. The thickness and length of the air-curtain nozzle were 0.1 m and 1.4 m, respectively. The velocity distributions due to the air-curtain were measured when the fans of the mechanical shaft were operated and not operated. Fig. 4 shows the velocity vector distributions in the tunnel without the train wind. There were similar velocity distributions in all the mechanical shafts. The developed air curtain can block the train wind in the tunnel when the air curtain velocity is 25 m/s.

In the numerical approach, a dust-collecting electrical precipitator was simulated as the air flowed through the porous zone. The air passed through the porous zone and experienced a pressure drop. A pressure drop and low velocity typically appeared in the porous zone. Fig. 3(b)) shows the porous zone location in the shafts. The dust collector in the middle of each shaft has filtering media with an effective filtration process. Filtration using porous filter media is important for the separation of airborne dust. Different filters are available, such as ash filters, metal fiber filters, and stainless filters with different porosity ratings. Porosity is defined by the fraction of the volume of voids divided by the total volume, and its random number ranges between 0 and 100%. The porosity of the electrical precipitator was assumed to be 70%. The structure of the porous zone had a porosity of 70%, which meant that 70% of the volume was available for air flow, and the remaining 30% was occupied by the solid material that comprises the structure. The mass flow rate with and without the porous zones in the shafts for the train-wind, the guide vane angle, and the velocity of the air curtain was 4 m/s, 60°, and 25 m/s, respectively, as shown in Table 2. The mass flow rate passing through the shafts decreased when the porous zone was installed in the shafts due to the blockage effect. A pressure drop occurred in the porous zone.

An electric precipitator (0.85 m × 0.8 m × 0.85 m) was installed in the middle of each ventilation shaft. Table 3 lists the experimental conditions for the particle concentration measurement and the results obtained from experimental and numerical analyses. The dirty air was pulled into the shaft by the

Table 2. The mass flow rates in the shafts with the guide vane installed and with/without porous zone.

| Mass flow rate, kg/s | Train-wind velocity, 4 m/s without porosity | Train-wind velocity, 4 m/s porosity 70 % |
|---|---|---|
| Tunnel inlet | 19.67 | 19.67 |
| Shaft 1 | 11.06 | 10.05 |
| Shaft 2 | 11.51 | 10.67 |
| Shaft 3 | 11.05 | 10.01 |

Table 3. Flow conditions, measured particle concentrations, and computational mass flow rate.

| | Shaft |
|---|---|
| Fans | 196.2 Pa |
| Train-wind | 4.0 m/s |
| Air-curtain | 25 m/s |
| Precipitator | 12 kV |
| Mass flow, kg/s (computed) | 11.06 |
| Particle size | 1 ㎛ |
| Particle concentration in the tunnel inlet | About 2000 mg/m$^3$ |
| Particle concentration: (measured) in DM | About 150 mg/m$^3$ |

axial-flow fan of the ventilation shaft with a capacity of 196.2 Pa. The velocities of the air curtain and train wind were 25 m/s and 4 m/s, respectively. The air curtain blocks the wake airflow behind the train in the tunnel, thereby increasing the amount of polluted air entering the precipitator. The applied voltage of the electric precipitator was 12 kV. The mass flow rate before the precipitator was 11.06 kg/s. The particle diameter was 1 ㎛. A particle concentration of 2000 mg/m$^3$ was generated at the tunnel inlet. A dust-monitoring device (Grimm Co. Germany) (DM) was installed in the tunnel between ventilation shafts 1 and 2 to monitor the particle concentration. The DM was operated for approximately 10 min for the analysis. The particle concentration at the DM was about 150 mg/m$^3$, which was found to have decreased by about 92.5% when the particle concentration at the DM was compared with the particle concentration at the tunnel inlet.

### *3.2 Effect of duct connections in the mechanical shaft of the real subway tunnel*

A mechanical shaft has an important role in the developed ventilation system. The mechanical shaft is used to discharge dusty air and to supply clean air to the tunnel. The mechanical shaft of a real tunnel was investigated numerically to apply the developed ventilation system. The twin-track subway tunnel, which waas chosen as the computational domain, is 100 m long with one mechanical shaft. The train wind was applied at track 1, and the same boundary conditions were applied to the computational domain. The mechanical shaft in the real tunnel was investigated by connecting ducts of the shaft.

Fig. 5 shows two ways of connecting ducts to apply the developed ventilation system in the tunnel. The existing mechanical shaft has three ducts: duct 1, an emergency duct, and duct 2. The emergency duct is the duct between duct 1 and duct 2, and is used in the developed ventilation system. There are two ways of connecting ducts: connecting duct 1 and duct 2, and connecting duct 1 and the emergency duct. The dusty air enters through duct 1 and passes through the electric precipitator, and the cleaned air from the precipitator enters the tunnel. The connected ducts were simulated with the real subway tunnel part. The performance of the connections was evaluated by the mass flow rate through the mechanical shaft. Axial-flow fans were installed in the ducts of the mechanical shafts. The velocity vector distribution and the mass flow rates in the mechanical shafts were computed. The velocity vector distributions in the shaft are shown in Fig. 6. The mass flow rate was measured at the precipitator installing location. The mass flow rates were 100.06 kg/s for the connection between

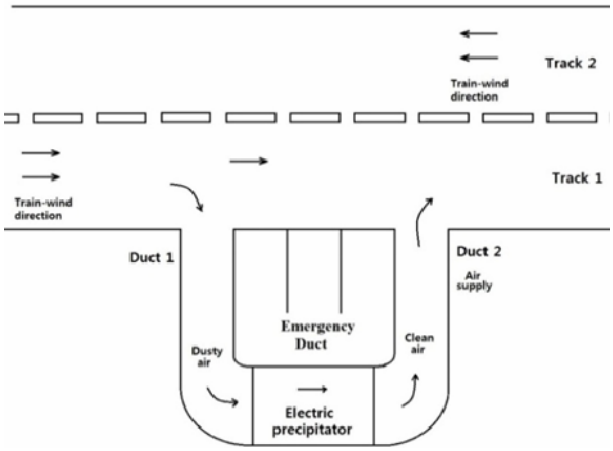


(a) Duct 1 and Duct 2

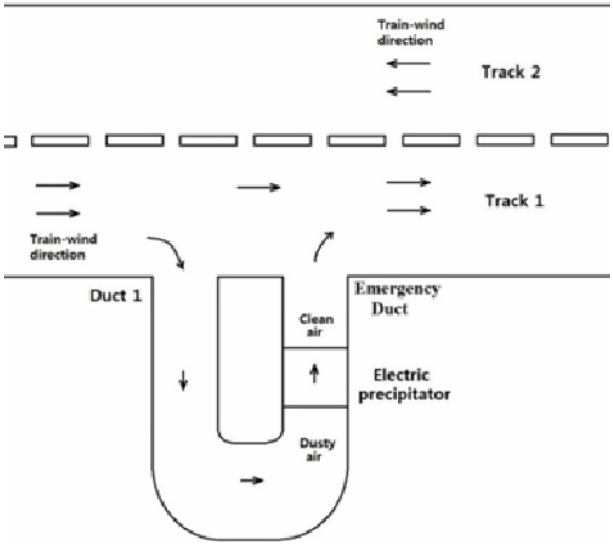


(b) Duct 1 and emergency Duct

Fig. 5. Schematic view of the shafts connections.

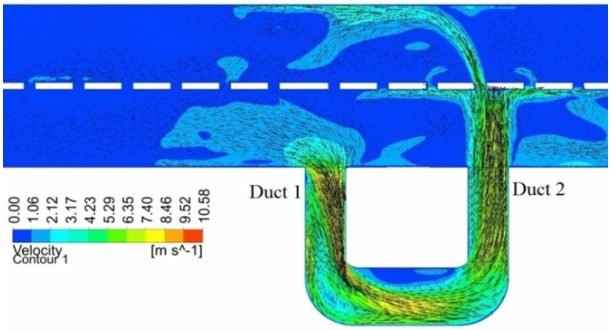


(a) Duct 1 and Duct 2

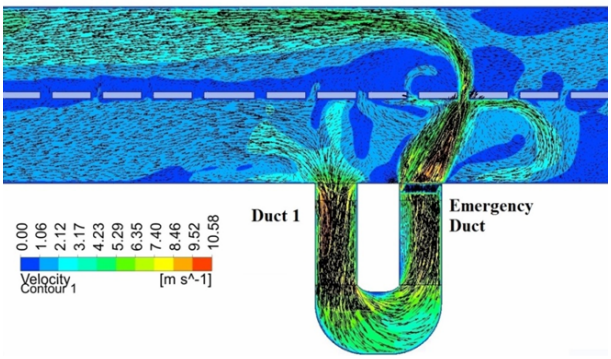


(b) Duct 1 and emergency Duct

Fig. 6. The velocity distributions in the tunnel and different connections between the mechanical shafts.

duct 1 and the emergency duct, and 93.89 kg/s for the connection of duct 1 and duct 2. The connection of duct 1 and the emergency duct was selected for further computations due to its larger mass flow rate.

### *3.3 Effect of installing the guide vane in the mechanical shaft*

Precipitators were used to reduce the amount of pollutants in the exhaust stream. They have a grid or baffle filter to remove large particulate from the exhaust air stream. Electrically charged grids charge most of the small particles passing them. The combination of grids creates a magnetic field where particles charged in the grid are repelled by the grid and are attached to the grounded collecting plates in the precipitator. The dust-collecting plates are removed regularly for cleaning. The efficiency of a precipitator is affected significantly by the airflow velocity and flow uniformity. The airflow at the precipitator could be controlled by the guide vanes for more homogeneous flow and thus higher efficiency. A precipitator was installed in the ducts of each ventilation shaft.

The real subway tunnel was investigated with guide vanes in the mechanical shaft and with train wind. The guide vanes were installed in the mechanical shaft to obtain more uniform flow before the electric precipitator, as shown in Fig. 7.

Guide vanes were installed on one side (at the corner) of the mechanical shaft, as shown in Fig. 8 and Table 4. The airflow entered duct 1 and was strongly rotated while it passed the

Table 4. The guide vane installation in the middle of the shaft (top view).

| | |
|---|---|
|  | 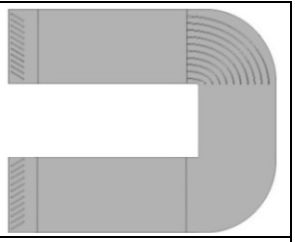 |
| 1 side Guide Vane 3 | 1 side Guide Vane 10 |
| 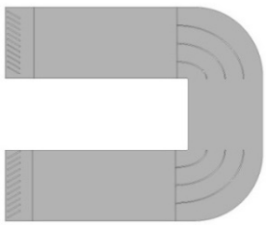 | 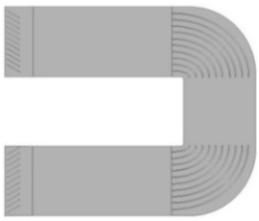 |
| 2 side Guide Vane 3 | 2 side Guide Vane 10 |

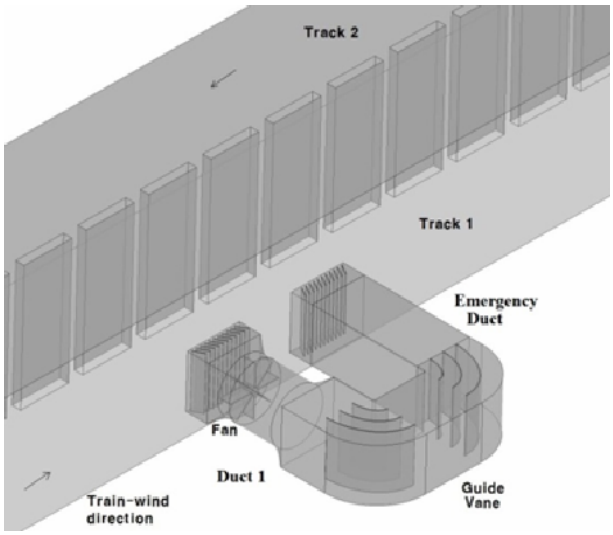


Fig. 7. The computational domain of the developed mechanical shaft of the real tunnel.

axial-flow fan of duct 1. A reverse airflow was formed in the center of duct 1, and the airflow moved forward passing by the installed guide vanes. High velocity was observed near the walls of the mechanical shaft in all cases. The airflow became homogeneous, and the backflow phenomenon around the corner was prevented significantly in the duct as the number of guide vanes increased. Fig. 9 shows the cross-sectional view after the guide vane, just before the electric precipitator.

Table 5 presents the mass average velocities at the divided guide vane zones. The average velocity was computed at each guide vane. The average velocity at A-A was high at the zones closest to the side walls of the mechanical shaft, especially at the inner walls. The average velocity across the guide vane zones was high when four guide vanes were installed.

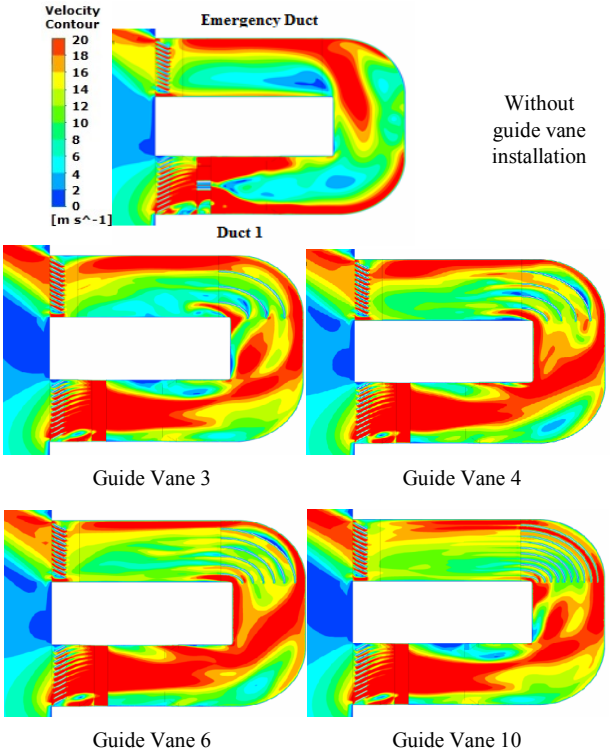


Fig. 8. The velocity contour distributions in the shaft for the one-side guide vane installations (top view).

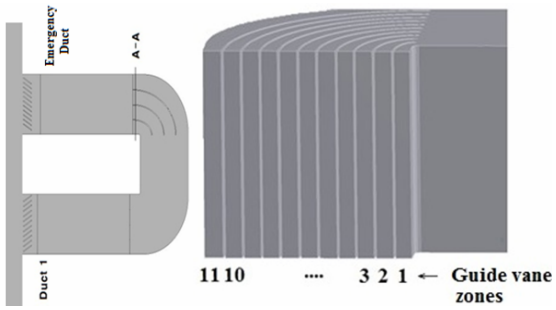


(a) Plane view (b) Cross-sectional view at A-A

Fig. 9. Cut-away view of the guide vane.

Fig. 10 shows the velocity distributions in the mechanical shaft when the guide vanes were installed on both sides (at the corners) of the shaft. The airflow entered and rotated strongly while passing the suction fan in duct 1. When the guide vanes were installed on both sides, the rotating airflow was suppressed significantly while passing the first guide vane zone and entering the second guide vane zone. The airflow after the second guide vane became relatively uniform. The guide vanes reduce the airflow speed and prevent the swirling airflow in the middle of the shaft. Homogeneous airflow was obtained when the guide vanes were installed on both sides at the corners. However, the low average velocity at the zones close to the wall due to boundary layer effects reduces the average velocity in the cross section. The average velocity was measured at A-A, where it was high at the center and low near

Table 5. The mass average velocity distributions and standard deviation at the exit of the guide vane zones (when the guide vane was installed at one side of the shaft), m/s.

| Guide vane zones (A-A cut) | Without guide vane | The numbers of the installed guide vane | | | |
|---|---|---|---|---|---|
| | | 3 | 4 | 6 | 10 |
| 1 | 14.4 | 18.49 | 14.55 | 18.63 | 9.31 |
| 2 | | 7.24 | 7.5 | 7.12 | 10.67 |
| 3 | | 11.18 | 13.5 | 11.0 | 11.54 |
| 4 | | 22.2 | 16.91 | 11.08 | 14.7 |
| 5 | | | 23.3 | 19.34 | 21.04 |
| 6 | | | | 11.3 | 10.9 |
| 7 | | | | 25.54 | 10.21 |
| 8 | | | | | 14.82 |
| 9 | | | | | 11.49 |
| 10 | | | | | 22.6 |
| 11 | | | | | 26.01 |
| Average velocity across the zones | 14.4 | 14.78 | 15.15 | 14.86 | 14.85 |
| Standard deviation | | 6.797845 | 5.725493 | 6.456455 | 5.748818 |

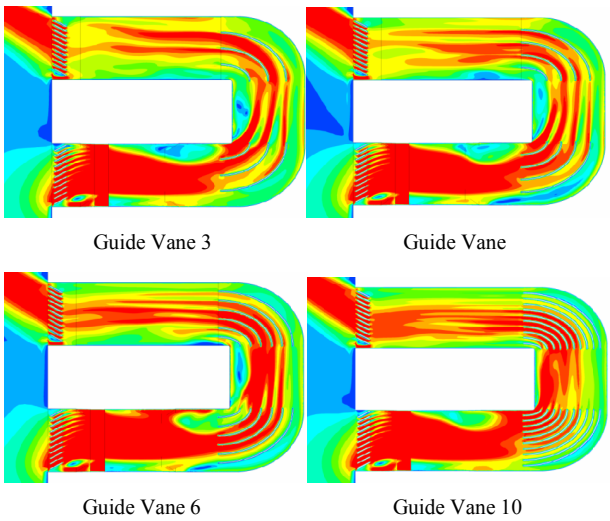


Fig. 10. The velocity contour distributions in the shaft for the two-side guide vane installations (top view).

the walls of the shaft, which is a typical homogeneous turbulent velocity profile. The turbulent flow was recovered after the second guide vane system.

Table 6 presents the average velocities across the guide vane zones. The average velocity across the guide vane zones became relatively similar as the number of guide vanes increased. The average velocity across the zones was slightly lower with three guide vanes than with more than three. The average velocity at the guide vane zones of the shaft was reduced when the guide vanes were installed on both sides only. Standard deviation of the velocity when the vanes were installed on one side and both sides of the shaft is presented in

Table 6. The mass average velocity distributions and standard deviation at the exit of the guide vane zones (when the guide vane was installed at both sides of the shaft), m/s.

| Guide vane zones (A-A cut) | Without guide vane | The numbers of the installed guide vane | | | |
|---|---|---|---|---|---|
| | | 3 | 4 | 6 | 10 |
| 1 | 14.4 | 8.157 | 8.63 | 8.60 | 6.31 |
| 2 | | 20.1 | 10.62 | 7.12 | 8.16 |
| 3 | | 13.19 | 22.68 | 11.0 | 9.18 |
| 4 | | 11.18 | 13.74 | 25.54 | 20.24 |
| 5 | | | 11.61 | 19.34 | 25.31 |
| 6 | | | | 11.3 | 13.79 |
| 7 | | | | 11.08 | 14.02 |
| 8 | | | | | 13.37 |
| 9 | | | | | 16.11 |
| 10 | | | | | 11.35 |
| 11 | | | | | 12.86 |
| Average velocity across the zones | 14.4 | 13.23 | 13.46 | 13.42 | 13.7 |
| Standard deviation | | 5.070005 | 5.475028 | 6.591527 | 5.436482 |

the tables. The lower standard deviation was 5.07 when three guide vanes were installed on both sides of the shaft.

Homogenization of the airflow in the shaft before the precipitator was much better with the installation of guide vanes on both sides than with guide vanes on one side. However, the cost of vane installation increases with the number of guide vanes. The proper guide vane installation was three guide vanes on both sides of the mechanical shaft, which provided similar flow quality at the lowest installation cost.

## 4. Conclusions

The air quality in a subway tunnel deteriorates due to air pollutants emitted from trains. Directly installing dust-removing systems such as electric precipitators inside an existing tunnel is impossible, although fire problems might arise as a result. The objective was to find a proper ventilation system and to apply the system to an existing subway tunnel. ANSYS CFX software was used for unsteady computations of the flow field in the subway tunnel by solving Reynolds-averaged Navier-Stokes equations.

First, the ventilation system was developed in a model tunnel by analyzing the airflow in the tunnel numerically and experimentally. The model subway tunnel was 54 m long, 1.65 m high, and 2.5 m wide. The ventilation performance was investigated by observing the mass flow rate through the mechanical shafts and the airflow in the tunnel. The effects of guide-vane angle, air curtain, and porous zone on the airflow in the shafts were studied in the model subway tunnel. The ventilation system developed was applied to an existing subway tunnel. The ducts of the mechanical shaft of the existing subway tunnel were connected to analyze the ventilation system in the tunnel. An existing emergency duct between the ducts of the mechanical shaft was used. The mass flow rate was higher with the mechanical shaft connection between duct 1 and the emergency duct than that when duct 1 and duct 2 were connected. The guide vanes were installed in the mechanical shafts before the electric precipitator to obtain uniform flow. Three guide vane installations on the both sides at the corners of the shaft gave better results with similar flow quality but lower cost of installation.

## Acknowledgment

This paper was supported by 2013 Yeungnam University post-doc Research Fund and 2013 Urban railroad technology development program fund by Ministry of Land, Transport and Maritime Affairs of Korean government.

## References

[1] J. S. Jeon, J. W. Seo, M. J. Jeon, S. W. Eom and Y. Z. Chae, Indoor Radon levels in the subway cabins of the Seoul metropolitan area, *Journal of Korean Society for Atmospheric Environment*, 28 (2012) 374-383 (in Korean).

[2] J. Modic, Fire simulation in road tunnels, *Tunnelling and Underground Space Technology*, 18 (2003) 525-530.

[3] T. Ogawa and K. Fujii, Numerical investigation of three-dimensional compressible flows induced by a train moving into a tunnel, *Computers & Fluids*, 26 (1997) 565-585.

[4] T. Y. Chen, Y. T. Lee and C. C. Hsu, Investigations of piston-effect and jet fan-effect in model vehicle tunnels, *J. of Wind Engineering and Industrial Aerodynamics*, 73 (1998) 99-110.

[5] J. Li, H. Peng and S. J. Li, Numerical simulation of flow characteristics in bidirectional subway tunnel, *Journal of Thermal Science and Technology*, 5 (2006) 331-334.

[6] F. Waymel, F. Monnoyer and M. J. P. William-Louis, Numerical simulation of the unsteady three-dimensional flow in confined domains crossed by moving bodies, *Computers & Fluids*, 35 (2006) 525-543.

[7] H. L. Karlsson, L. Nilsson and L. Moller, Subway particle are more genotoxic than street particles and induce oxidative stress in cultured human lung cells, *Chem. Res. Toxicol*, 18 (2005) 19-23.

[8] J. Song, H. Lee, S. Kim and D. Kim, How about the IAQ in subway environment and its management?, *Asian J. of Atmospheric Environment*, 2-1 (2008) 60-67.

[9] ANSYS CFX, ANSYS Workbench, ICEM-CFD, CFX-Pre, CFX-Solver, *CFX-Post User's Manual* (2009).

[10] S. Gupta, M. Pavageau and J. C. Elicer-Cortes, Cellular confinement of tunnel sections between two air curtains, *Building and Environment*, 42 (2006) 3352-3365.

[11] M. Juraeva, K. J. Ryu, S. H. Jeong and D. J. Song, Influence of mechanical ventilation-shaft connecting location on subway tunnel ventilation performance, *J. of Wind Engineering and Industrial Aerodynamics*, 119 (2013) 114-120.

[12] F. R. Menter, Two-equation eddy-viscosity turbulence models for engineering applications, *AIAA-J.*, 32 (1994) 269-289.
[13] D. C. Wilcox, Comparison of two equation turbulence models for boundary layers with pressure gradient, *AIAA Journal*, 31 (9) (1993) 1414-1421.
[14] M. Juraeva, K. J. Ryu, S. H. Jeong and D. J. Song, A computational analysis of the airflow in a twin-track subway tunnel with a sliding-curtain to improve ventilation performance, *J. of Mechanical Science and Technology*, 27 (8) (2013) 2359-2365.

**Dong Joo Song** received his B.S. degree in Seoul National University, and his M.S. and Ph.D. degrees in Aerospace engineering, Virginia Tech. He is now a professor at School of Mechanical Engineering, Yeungnam University. Professor Song's research interests include CFD, Thermofluid system design, and aerodynamics.